Atomistic Simulation of Band-to-Band Tunneling in SiGe: Influence of Alloy Scattering

Hong-Hyun Park[1*], Seonghoon Jin[1], Woosung Choi[1],
Mathieu Luisier[2], Jongchol Kim[3], and Keun-Ho Lee[3]
[1]Device Laboratory, Samsung Semiconductor Inc., San Jose, California, USA
[2]Integrated Systems Laboratory, ETH Zurich, Zurich, Switzerland
[3]Semiconductor R&D Center, Samsung Electronics, Hwasung-si, Gyeonggi-do, Korea
*e-mail: honghyun.p@samsung.com

***Abstract*—We present atomistic simulation results of band-to-band tunneling (BTBT) in SiGe random alloy. We use the non-equilibrium Green's function (NEGF) method to extract BTBT generation rates for different mole fractions, crystal orientations, and electric field strengths. The results show that alloy scattering plays an important role in the indirect BTBT of SiGe alloy and should not be neglected. Also, we improved the analytical BTBT model based on the atomistic simulation results.**

Keywords—SiGe, random alloy, band-to-band tunneling; quantum transport; non-equilibrium Green's function (NEGF), tight-binding, valence force field (VFF)

I. Introduction

The off-state of ultra-scaled semiconductor field-effect transistors (FETs) can be vulnerable to BTBT leakage. As shown in Fig. 1(a), the high electric field applied at the channel-drain junction results in thin and low tunneling barrier, which induces electrons tunneling from the filled states of the valence band (VB) to the empty states of the conduction band (CB). As the doping levels become higher for sub-10nm FETs, BTBT is considered as one of the significant off-current leakage sources.

As Ge and SiGe are studied as channel materials in hopes of higher carrier mobility values than those of Si, the concern of BTBT leakage is also growing since Ge is known to be more vulnerable to BTBT than Si. There are two major differences between the BTBT in Si and Ge. First, Ge has a smaller band-gap than Si as shown in Fig. 1(b). Under the same electric field, a smaller band-gap means thinner and lower tunneling barrier. Second, BTBT in Ge is dominated by direct tunneling from the VB to the Γ valley in the CB while BTBT in Si requires involvement of electron-phonon (e-ph) interactions because the VB at Γ and the six valleys in the CB at Δ have different transverse crystal momentums.

BTBT in SiGe alloy can involve both the direct and the indirect transitions depending on the Ge mole fraction. While the direct BTBT is solely determined by the band structure, the indirect BTBT is proportional to the scattering processes that result in inter-valley transitions. It is well known that the random alloy scattering can give a significant impact on the carrier mobility in SiGe. However, the influence of the alloy scattering on BTBT is not understood and considered so far. Hence, in this paper we perform fully atomistic quantum simulations to see the effect of random alloy on BTBT quantitatively. Also, we improve the analytical BTBT model by taking into account alloy scattering [1].

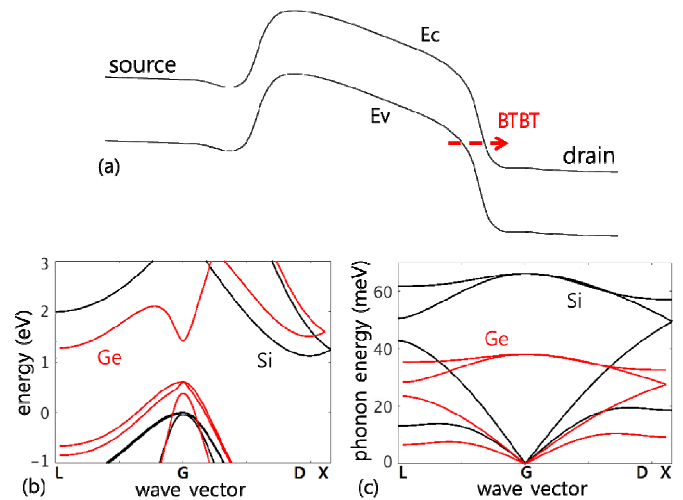

Fig. 1. (a) Schematic band diagram of an n-type FET in off-state operation (low V_G and high V_D), where BTBT leakage can happen at the channel-drain junction. (b) Electronic bandsturctures of Si and Ge calculated by the tight-binding method. For Si, E_v = 0.0 eV, $E_{c,\Delta}$ = 1.12 eV, $E_{c,L}$ = 1.99 eV. For Ge, E_v = 0.6 eV, $E_{c,L}$ = 1.27 eV, $E_{c,\Gamma}$ = 1.41eV, $E_{c,\Delta}$ = 1.50 eV. (c) Phonon bandsturctures of Si and Ge calculated by the valence force field method.

II. Simulation Method

In order to account for the electronic transport in SiGe alloy we employ the atomistic NEGF approach based on the empirical tight-binding method with Boykin's strain model [2, 3]. We also use the valence force field (VFF) method to solve the mechanical properties of atomistic structures such as strain/stress and phonon [4]. All the parameters required by the models are calibrated against bulk Si and Ge materials separately as shown in Figs. 1(b) and 1(c) and we do not perform additional fittings for SiGe alloy nor calibration by device-level simulations [5]. The applicability of the parameters for SiGe alloy is also validated. Fig. 2(a) shows that the band edges extracted from random alloy simulations agree

© 2017 The Japan Society of Applied Physics

well with those from experimental data for all the mole fraction. Fig. 2(b) shows the phonon bandstructure of $Si_{0.1}Ge_{0.9}$ random alloy. Interestingly, some high energy bands similar to those of Si are still observed in this Ge-rich material. These bands are confirmed to be in good agreement with density functional theory simulations.

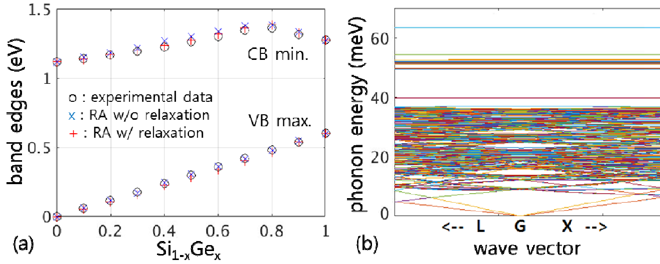

Fig. 2 (a) Comparison between the calculated and the experimentally observed CB and VB edges of bulk SiGe according to the Ge mole fraction. Our model parameters calibrated against bulk Si and Ge materials also give good agreements for SiGe alloy. Slightly better agreements can be obtained when the alloy structures are relaxed by the VFF method. (b) Phonon bandstructure of a supercell $Si_{0.1}Ge_{0.9}$ alloy calculated by the VFF method.

The effect of electron-phonon scattering in SiGe is modelled rigorously based on the deformation potential theory [6]. In the model the information of phonon is obtained from the VFF simulation and its influence on the electronic system is captured by the TB model. The scattering calculation does not require any fitting parameters, and the validity of the model is demonstrated by calculating the phonon-limited mobility values of Si and Ge [5].

As a first step of the simulation, we prepare an atomistic SiGe structure for a given mole fraction. For example, Fig. 3(a) shows a simulation domain for $Si_{0.5}Ge_{0.5}$ where Si and Ge atoms are randomly generated according to a given mole fraction and placed at their virtual lattice sites. The transport direction is set to x axis while periodic boundary conditions are applied along y and z axes. Note that the simulation setting is just an approximation to a bulk system and may result in artificial variations in the simulation results because of the randomness within the finite simulation domain. Hence, it is desirable to prepare as big simulation domain as possible.

Once a disordered structure is constructed, we relax its atom positions using the VFF method to obtain correct internal strain field in the case of SiGe alloy. This relaxation process improves the accuracy of the following atomistic NEGF simulations as shown in Fig. 2(a).

Now we perform NEGF simulations. To mimic the transport in bulk material under a uniform electric field, the electrostatic potential profile is precalculated and the Fermi levels are set as shown in Fig. 3(b). In this case electrons are transported from the VB in the left to the CB in the right. Once an NEGF simulation is done, the BTBT generation rate can be estimated as the calculated BTBT current divided by the effective tunneling length (L_{eff}) which is explained in Fig. 3(b). Actually, this approach is an approximation to an infinitely long system with a uniform electric field. For more accurate calculations, the contact self-energy functions of the NEGF solver should be modified for the periodicity along the transport direction but it is not covered in this paper. Also, note that the calculated BTBT current has artificial variation according to the configuration of SiGe random alloy. The calculated BTBT current values from ensemble simulations are more like a log-normal distribution than a normal distribution as shown in Fig. 3(c) because BTBT current is exponentially proportional to the Ge mole fraction. We take the mean value of the log-normal distribution of ensemble simulations as a representative BTBT current.

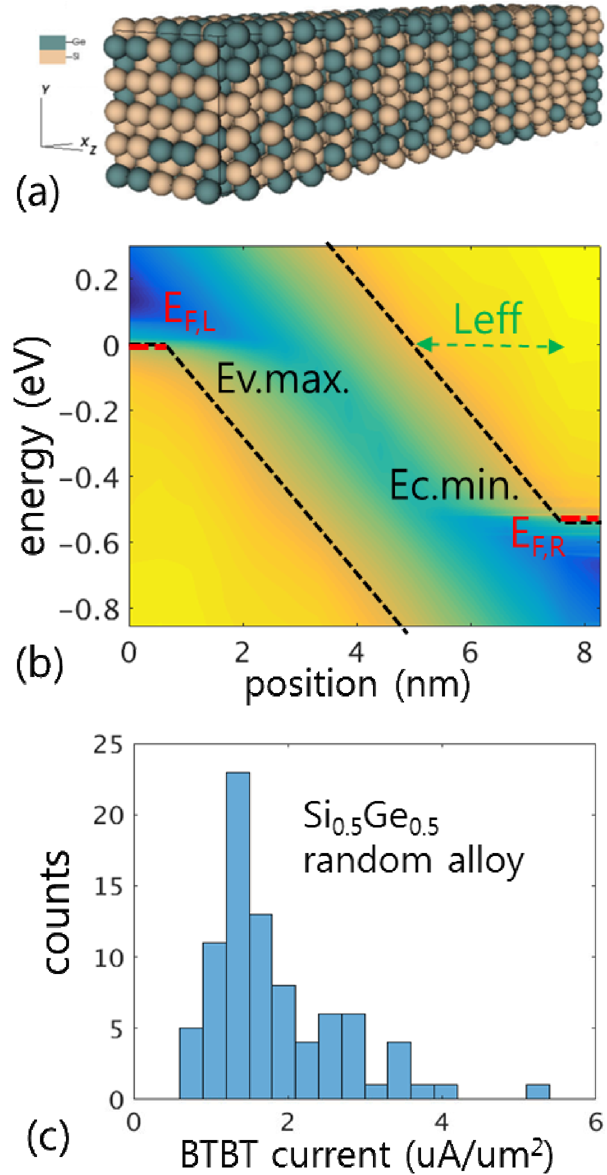

Fig. 3 (a) Example atomistic structure for BTBT simulation of $Si_{0.5}Ge_{0.5}$ random alloy. (b) Density-of-states spectrum and schematic diagram showing how the simulation conditions are prepared for a given electric field strength. (c) Distribution of the calculated BTBT current from 84 samples of $Si_{0.5}Ge_{0.5}$ random alloy. This current variation is not physical but artificial resulted from the random configurtion of Si and Ge atoms in the finite size of simulation domain.

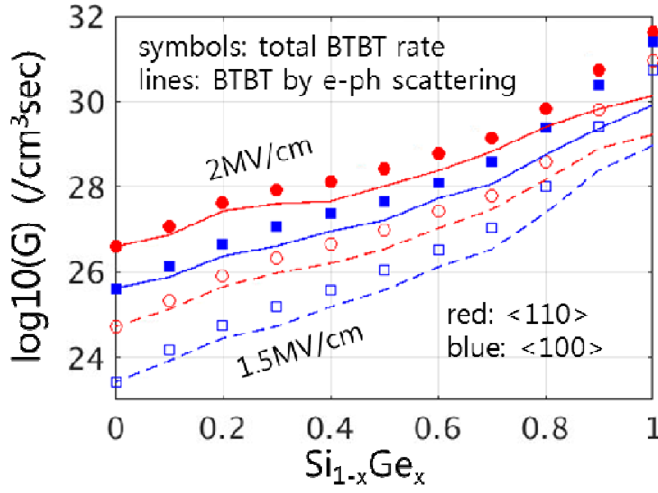

Fig. 4. Simulated BTBT generation rates in bulk SiGe alloy as a function of Ge mole fraction. The BTBT rates are represented as filled symbols and solid lines at 2 MV/cm of electric field and empty symbols and dashed lines at 1.5 MV/cm of electric field, respectively.

III. Simulation Results

Atomistic simulation results are summarized in Fig. 4, where BTBT generation rates in SiGe alloy are plotted for different Ge mole fractions, crystal orientations, and electric field strengths. As expected, BTBT in SiGe is very sensitive to the Ge mole fraction e.g. BTBT in Ge is higher than that of Si by five orders of magnitude. For pure Si the total BTBT rate and its partial contribution by e-ph scattering are the same, which confirms that the BTBT in Si is determined by the inter-valley e-ph scattering mechanisms. For SiGe with very high Ge mole fraction the contribution of e-ph scattering is very small compared to the total BTBT, which confirms that BTBT is mainly due to the direct tunneling. For the other mole fractions of SiGe the indirect BTBT is the main tunneling mechanism where both of alloy and e-ph scattering have significant effects.

Overall, BTBT along <110> direction shows higher rates than <100> direction. The insensitivity of the BTBT in pure Ge to the crystal orientation can be understood by the isotropy of the Γ valley of its CB. Also, as expected, BTBT is sensitive to the magnitude of electric field. The sensitivity is higher for Si but lower for Ge mainly because of the difference in their band-gaps.

IV. Analytical BTBT model

Based on the atomistic simulation results, the analytical BTBT model is improved by taking into account the effect of alloy scattering. The results of the atomistic simulations and the improved analytical model are compared in Fig. 5. Once its parameters are calibrated properly, the analytical model gives good agreements with the atomistic simulations for various combinations of mole fractions, crystal orientations, and electric field strengths. We believe that more fine tuning of the parameters can give better matching.

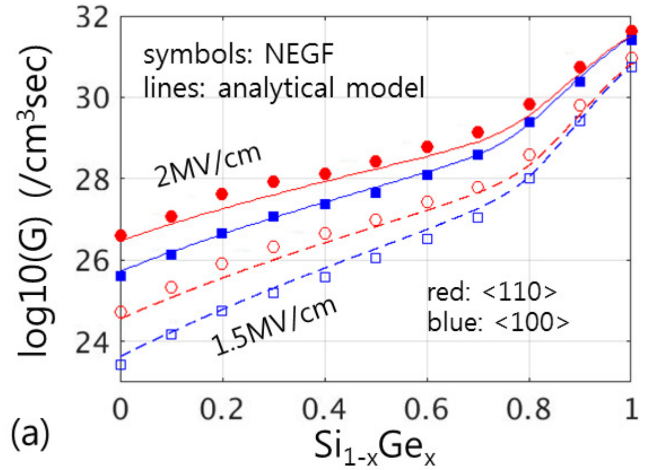

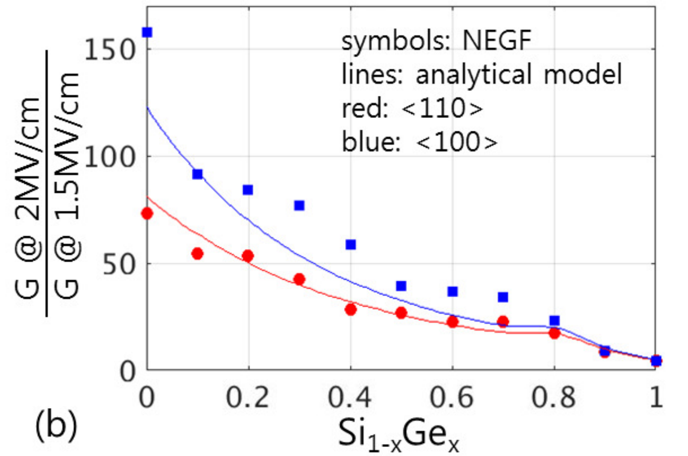

Fig. 5. Comparisons between atomistic simulations (symbols) and the analytical BTBT model (lines) whose parameters are calibrated against the atomistic BTBT simulation results. (a) BTBT generation rates vs. Ge mole fraction with the symbols and lines representing the same as in Fig. 4. (b) Sensitivity of BTBT rates to the electric field strength.

In the following, the improved analytical BTBT model is introduced briefly for the sake of completeness. A more detailed explanation can be found in [1]. The model computes the BTBT generation rate (G_{BTBT}) which is a kind of material property that indicates how many electrons are generated by BTBT per unit volume and unit time under the limit of uniform electric field. For SiGe it can be modelled as [7-11]

$$G_{BTBT} = \sum_i A_i \left(\frac{F}{F_0} \right)^{P_i} \cdot \exp\left(-\frac{1}{qF} \int_{E_V}^{E_{C,i}} \kappa_{VC,i}(E) dE \right) \quad (1)$$

, where i is the CB valley index (i = Γ, six Δ, and four L valleys), F is the magnitude of electric field, F_0 = 1 MV/cm, P_i is a fitting parameter, q is the elementary charge. $\kappa_{VC,i}$ is the imaginary wavenumber between the VB edge (E_V) and the edge of the CB valley i ($E_{c,i}$), which can be computed from full-band simulations. For the coherent tunneling A_i is given by [9-10]

$$A_i = \frac{g \pi m_{r,i}^{1/2} (qF_0)^2}{9h^2 E_{G,i}^{1/2}} \quad (2)$$

, where g is the spin degeneracy, $E_{G,i} = E_{C,i} - E_V$, $m_{r,i}$ is the tunneling mass, and $h=2\pi\hbar$ is the Plank constant. For the indirect tunneling, A_i is given by [7,8,10]

$$A_i = \frac{g (m_V m_{C,i})^{3/2} (qF_0)^{5/2}}{2^{17/4} h^{7/2} m_{r,i}^{5/4} E_{G,i}^{7/4}} C_{scat} \quad (3)$$

, where m_V and $m_{C,i}$ are the density-of-states effective masses for the VB and the CB valley, respectively. Taking into account the phonon and alloy scattering mechanisms, the coupling constant C_{scat} can be written as [1]

$$C_{scat} = \frac{(1+2N_{op}) h D_{op}^2}{2\rho E_{op}} + \frac{\pi \Omega_{cell} U_{alloy}^2 (1-x) x}{4\hbar} \quad (4)$$

, where ρ is the mass density, x is the Ge mole fraction, D_{op} is the deformation potential, E_{op} is the phonon energy, N_{op} is the phonon occupation, Ω_{cell} is the volume of unit cell, and U_{alloy} is the alloy scattering potential. We notice that U_{alloy} is smaller than the alloy potential used in the carrier mobility calculation, which is because only inter-valley transitions among all alloy scattering can contribute to the indirect BTBT.

V. CONCLUSION

In this paper atomistic NEGF simulations are performed to investigate the BTBT in SiGe alloy. The BTBT generation rate is quantitatively estimated for different Ge mole fractions, crystal orientations, and electric field strengths. It is found that not only electron-phonon scattering but also alloy scattering plays an important role in indirect BTBT. Based on the atomistic simulation results, the analytical BTBT model is improved by taking into account the effect of alloy scattering.

REFERENCES

[1] Seonghoon Jin, Hong-Hyun Park, Mathieu Luisier, Woosung Choi, Jongchol Kim, and Keun-Ho Lee, "Band-to-Band Tuenneling in SiGe: Influence of Alloy Scattering," IEEE Electron Device Letters, vol. 38, no. 4, pp. 422-425, 2017.

[2] J. C. Slater and G. F. Koster, "Simplified LCAO Method for the Periodic Potential Problem," Physical Review, vol. 94, no. 6, pp. 1498-1524, June 1954.

[3] Timothy B. Boykin, Mathieu Luisier, Mehdi Salmani-Jelodar, and Gerhard Klimeck, "Strain-induced, off-diagonal, same-atom parameters in empirical tight-binding theory suitable for [110] uniaxial strain applied to a silicon parameterization," Physical Review B, vol. 81, p. 125202, 2010.

[4] Abhijeet Paul, Mathieu Luisier, and Gerhard Klimeck, "Modified valence force field approach for phonon dispersion: from zinc-blende bulk to nanowires," J. Comput Electron, vol. 9, pp. 160-172, 2010, doi: 10.1007/s10825-010-0332-9.

[5] Hong-Hyun Park, Yang Lu, Woosung Choi, Young-Tae Kim, Keun-Ho Lee, and Youngkwan Park, "Atomistic simulations of phonon- and alloy-scattering-limited mobility in SiGe nFinFETs," in International Conference on Simulation of Semiconductor Processes and Devices (SISPAD), pp. 257-260, Sep. 2014.

[6] Mathieu Luisier and Gerhard Klimeck, "Atomistic full-band simulations of silicon nanowire transistors: Effect of electron-phonon scattering," Physical Review B, vol. 80, 155430, 2009.

[7] L. V. Keldysh, "Behavior of non-metallic crystals in strong electric fields," Soviet J. Experim. Theoretical Phys., vol. 6, no. 4, pp. 763–770, Apr. 1958.

[8] L. V. Keldysh, "Influence of the lattice vibrations of a crystal on the production of electron-hole pairs in a strong electrical field," Soviet J. Experim. Theoretical Phys., vol. 7, no. 4, pp. 665–669, Oct. 1958.

[9] E. O. Kane, "Zener tunneling in semiconductors," J. Phys. Chem. Solids, vol. 12, no. 2, pp. 181–188, 1960.

[10] E. O. Kane, "Theory of tunneling," J. Appl. Phys., vol. 32, no. 1, pp. 83–91, 1961.

[11] G. A. M. Hurkx, D. B. M. Klaassen, and M. P. G. Knuvers, "A new recombination model for device simulation including tunneling," IEEE Trans. Electron Devices, vol. 39, no. 2, pp. 331–338, Feb. 1992, doi: 10.1109/16.121690.